Enhanced thermal stability of a lithiated nano-silicon electrode by fluoroethylene carbonate and vinylene carbonate

Irina A. Profatilova*, Christoph Stock, André Schmitz, Stefano Passerini, Martin Winter**

MEET Battery Research Center, Institute for Physical Chemistry, University of Muenster, Corrensstrasse 46, 48149 Muenster, Germany

HIGHLIGHTS

► The thermal behavior of a nano-Li_xSi anode in electrolytes has been investigated.
► The thermal runaway is delayed by ~50 °C in the presence of FEC and VC additives.
► We identified two mechanisms of Li_xSi protection by the additives during heating.
► FEC and VC electrochemically generate a thermally stable SEI covering the Li_xSi.
► A robust "secondary SEI" is formed by thermal degradation of FEC and VC.

GRAPHICAL ABSTRACT
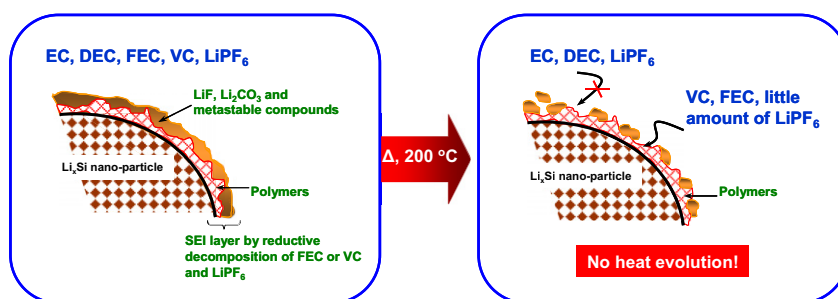
ABSTRACT

The thermal behavior of the fully lithiated nano-silicon electrode in contact with an 1 M $LiPF_6$ in EC/DEC electrolyte is investigated by differential scanning calorimetry (DSC) in the absence and presence of fluoroethylene carbonate (FEC) and vinylene carbonate (VC) electrolyte additives. In the additive-free electrolyte, intense exothermic reactions commence at approximately 153 °C when in contact with Li_xSi. At contrast, the onset temperature of the thermal runaway is shifted to 200 °C and 214 °C when the charged Li_xSi is heated in the presence of FEC and VC in the electrolytes, respectively. The mechanism of this thermal stability improvement by FEC and VC is studied using attenuated total reflection Fourier transform infrared spectroscopy (ATR-FTIR) and by specific measures to design the SEI on the surface of the nano-Si particles. The additives form a robust "primary SEI" on the surface of the Li_xSi particles during the first charge that is rich in polycarbonate species and stable at elevated temperatures. In addition, the thermal degradation of FEC and VC in the electrolyte solution yields a highly resistive "secondary SEI" on the electrode surface that covers the lithiated silicon electrode (together with the "primary SEI") and protects it from thermal runaway up to 200 °C.

© 2012 Elsevier B.V. All rights reserved.

1. Introduction

The stringent safety requirements for large-scale lithium-ion batteries (LIBs) are some of the main obstacles slowing down their commercialization for electric vehicle and stationary applications. Over the last decades, active development of the LIB technology has markedly enlarged the technology's specific energy; increased amounts of energy can now be stored per unit of LIB mass [1–4].

---

* Corresponding author. CEA/LITEN, Commissariat a l'Energie Atomique/Laboratoire d'Innovation pour les Technologies des Energies Nouvelles, 17 rue des Martyrs, 38054 Grenoble Cedex 9, France. Tel.: +33 04387 822 45; fax: +33 04387 843 83.
** Corresponding author.
E-mail addresses: irishkapro@mail.ru, irina.profatilova@cea.fr (I.A. Profatilova), martin.winter@uni-muenster.de (M. Winter).

Because the electrolytes used in LIBs are usually volatile and flammable [5–8] and the active electrode materials are either highly reducing or highly oxidizing agents in a charged state, the risk of a thermal runaway is of major concern. Since the first lithium-ion battery, which was based on petroleum coke/LiCoO$_2$ chemistry, was commercialized in 1990 by Sony Co. [9], a number of accidents related to this technology have been reported each year, including the spontaneous fire or explosion of LIBs and LIB packs [10]. Heat distribution and transfer within a lithium battery can be controlled by engineering measures, such as the proper design of electrodes and cells as well as monitoring of the cell conditions [11]. Vents and current-interrupt devices (CIDs) can be added to respond to a sudden increase in pressure, current flow, temperature, etc. [1,10]. Yet, sometimes these devices still prove insufficient for preventing fast-rate exothermic reactions between the cell components. For this reason, major attention must be paid to the prevention of thermally induced reactions inside batteries [12,13] and the cell chemistry needs to be designed in a way that the impact of thermal reactions on the safety of the cell is minimized.

Lithium storage metals, such as Si, Sn, etc., have been extensively studied since decades [14–16]. Usually, nano-sized and nanostructured materials lithium storage active material and composites are applied, as they show better cycling behavior [17–20]. Nano-sized silicon continues to be extensively studied as an active material for negative electrodes in LIBs. The superior specific capacity (approximately 3500 mAh g^{-1} during long-term cycling [21]) of nano-sized silicon, along with its abundance on earth and non-toxicity, makes it very attractive for use as an electrode material in LIBs [22–25]. The fabrication of nano-sized morphologies allowed LIB technology to overcome the low electronic and ionic conductivity problems frequently associated with Si-based electrode materials [26] and also to alleviate the volume expansion problem related the strong structural changes during Li insertion and contraction [27–29]. Researchers have been rather enthusiastic about the synthesis of nano-silicon in a variety of morphologies (including powders, tubes, fibers, rods, electrodeposits, various composites with graphite) and by the electrochemical properties of electrodes using nano-silicon [22–25,30–35]. However, the thermal stability of the nano-silicon electrode, when in contact with the electrolytes used in LIBs, has been minimally explored [36,37]. The electrochemical reactivity of lithium storage metals and alloys with the electrolyte is different to that of graphite [38–41]. This is also true for the thermal stability. Our previous study was focused on the thermal decomposition mechanism of lithiated nano-silicon electrodes in contact with EC/DEC 1 M LiPF$_6$ electrolytes; these studies were carried out with a combination of DSC and ATR-FTIR spectroscopy methods [37]. It was found that the thermal reactions between the lithiated silicon electrode and the electrolyte were initiated at approximately 77 °C, although the largest amount of heat was generated between 150 and 300 °C. The origin of the exothermic peaks in the DSC thermograms was identified with ATR-FTIR spectroscopy. The role of the electrolyte salts LiPF$_6$ and LiTFSI in the thermal stabilization of Li$_x$Si was also elucidated.

The importance of the solid electrolyte interphase (SEI) layer that is formed predominantly on the surface of the negative electrode, which has operating potentials below the thermodynamic stability window of the organic electrolyte solution, is well recognized today. The chemical structure and morphology of the SEI layer can critically influence the safety, cycle life, power capability, side reactions and shelf life of a LIB [42–47]. The use of electrolyte additives effectively enables modifications to the electrochemical and thermal properties of the electrolyte/electrode interface. The SEI-forming electrolyte additives readily decompose on the electrode surface via an electrochemical process, which occurs prior to the decomposition of the main electrolyte components, such as EC and LiPF$_6$, and thus forms a robust protective film [48–52]. This process is favored by the low energy level of the lowest unoccupied molecular orbital (LUMO) resulting from the chemical structure of the additive [53,54]. Structural modifications of the ethylene carbonate molecule with a double bond (giving VC) or substitution of the halogen atoms (giving FEC) can both cause large decreases in the LUMO level [53]. Numerous works have reported improvements of the electrochemical properties of conventional graphite anodes via the introduction of VC or FEC to the electrolyte solution [53–64]. Moreover, these additives have been successfully implemented in the silicon-based electrode and further increase its cycle life [65–68]. Although unsaturated and halogenated organic carbonates are well known to be effective SEI-forming electrolyte components for use in LIBs [69–71], their protective function at elevated temperatures has only been recognized recently. Herstedt et al. investigated the thermal stability of graphite after cycling in a VC-containing electrolyte using the DSC method [72]. They found that the onset temperature of the exothermic reaction of the electrode was shifted from 70 °C to 110 °C when cycled in the presence of an additive. This effect was caused by the formation of a polymeric species on the electrode surface and a small amount of salt products that were observed in the composition of the VC-derived SEI layer. Lee et al. described the function of vinylene carbonate (VC) for the protection of graphite electrodes based on cycling analyses carried out at 80 °C. The enhanced cycling performance of graphite in the presence of 2 wt% VC was ascribed to the formation of a polyvinylene carbonate-based SEI layer on the electrode surface [73]. The thermal stability of the EC/EMC 1.1 M LiPF$_6$ electrolyte was improved via the incorporation of 1 wt% VC [59]. Fluoroethylene carbonate was successfully used for the enhanced cycling stability of a silicon nanowire anode and a LiMn$_2$O$_4$/graphite cell analyzed in an alkyl carbonate electrolyte solution at 60 °C [68,74]. Previously, we have described an improvement to the thermal resistivity of graphite when in contact with an electrolyte via the introduction of FEC into the EC/EMC 1 M LiPF$_6$ solution, both with and without the use of ionic liquids [75,76]. The central stage in all the works listed above was taken by the specific chemical composition of the SEI layer that was formed by the ethylene carbonate derivatives, as the composition affected both the cycling performance and the thermal stability of the lithium-ion cells. However, the thermal decomposition mechanism of the carbonate-based electrolyte additives that were in contact with the electrodes in the LIBs has not yet been comprehensively explored. In fact, there have been no investigations on the high-temperature stability of nano-sized silicon in contact with electrolytes that contain unsaturated or halogenated ethylene carbonate derivatives.

This work intends to fill the gap in the literature by revealing the role of VC and FEC as electrolyte components in the thermal reactions between the lithiated silicon nano-powder and the carbonate-based electrolyte when using the DSC method. Our main interest is in the factors that are responsible for initiating the generation of exothermic heat. The mechanism of lithiated silicon protection at elevated temperatures is proposed based on SEI modeling experiments and ATR-FTIR observations.

2. Experimental

The details of the Si nano-powder synthesis procedure were reported in our previous work [37]. A Si-based electrode was prepared by mixing 80 wt% Si nano-particles, 8 wt% Super-P (Timcal, Switzerland) and 12 wt % sodium carboxymethyl cellulose (Na CMC, Dow Wolff Cellulosics, Germany) aqueous solution in an Ultra-Turrax dispenser. The resulting slurry was cast onto a Cu

foil with a Doctor Blade coater, which had its height setting adjusted to 120 μm. The electrode was pre-dried at 80 °C for 1 h before being punched and further dried at 120 °C in a vacuum oven for 20 h. The mass loading of the electrode was approximately 1.7 mg cm^{-2}.

The electrochemical lithiation of the Si-based electrodes was conducted in a three-electrode Swagelok cell with Li metal used for both the counter and reference electrodes and employing a Maccor S4000 Battery Tester. The compositions of the electrolyte solutions used in this investigation are presented in Table 1. A constant current of 0.1 C (around 0.4 mA) was applied to lithiate the Si active material. After the voltage reached 5 mV vs. Li/Li$^+$, a constant voltage step was carried out until the current had dropped to 0.02 C. The X-ray diffraction analysis of the resulting Li$_x$Si phases has been shown previously [37]. After the charging (lithiation) step, the cells were carefully opened in a dry room with a D.P. < −70 °C, and the retrieved Si-based electrodes were rinsed in dimethyl carbonate (DMC) and then dried under vacuum for 20 min. A total of 2 mg of a scratched-off electrode material were further sealed in hermetic high-pressure DSC pans (TA, USA) with the electrolyte, which was 40 wt% that of the Li$_x$Si. The DSC measurements were conducted with a DSC Q2000 (TA, USA) at a temperature ramp of 2 °C min^{-1}. When necessary, the DSC cells were opened in a glove box with both the oxygen and moisture contents measuring less than 1 ppm, and the retrieved active material was directly transferred to a hermetic ATR Golden Gate unit for the subsequent ATR-FTIR measurements. The ATR-FTIR spectra were recorded under a nitrogen atmosphere using a Vertex 70 (Bruker Optik, Germany) with a resolution of 4 cm^{-1}.

3. Results and discussion

3.1. Electrochemical properties of the silicon-based electrode

The electrochemical lithiation of the nano-Si electrode was conducted prior to measuring the thermal stability. Fig. 1(a) illustrates the typical charge curves obtained for the Si-based electrode in different electrolytes. The specific capacity was slightly higher for the Ref electrolyte without additive (3875 mAh g^{-1}) than for the Si electrodes, which were cycled in FEC10 and VC10 and delivered capacities of 3750 and 3776 mAh g^{-1}, respectively (see Table 1 for the electrolyte abbreviations). Examination of the differential capacity graphs in the vicinity of the SEI layer formation potentials (Fig. 1(b)) shows that the reductive decomposition of the Ref electrolyte component yielded two pronounced peaks centered at 830 and 400 mV vs. Li/Li$^+$. The electrochemical reduction reactions of electrolytes containing additives tend to be less intense, and the peaks of the additive decompositions can be observed at 1110 mV vs. Li/Li$^+$ for FEC10 and at 1000 mV vs. Li/Li$^+$ VC10. The peaks at approximately 400 mV vs. Li/Li$^+$ are also considerably decreased by the introduction of the additives. This observation confirms that FEC and VC both decompose on the surface of the Si-based electrode and form a proper protective film in an early stage of the 1st charge, which restricts further electrochemical reduction of the main electrolyte components.

Table 1
Compositions of the electrolytes used in this work.

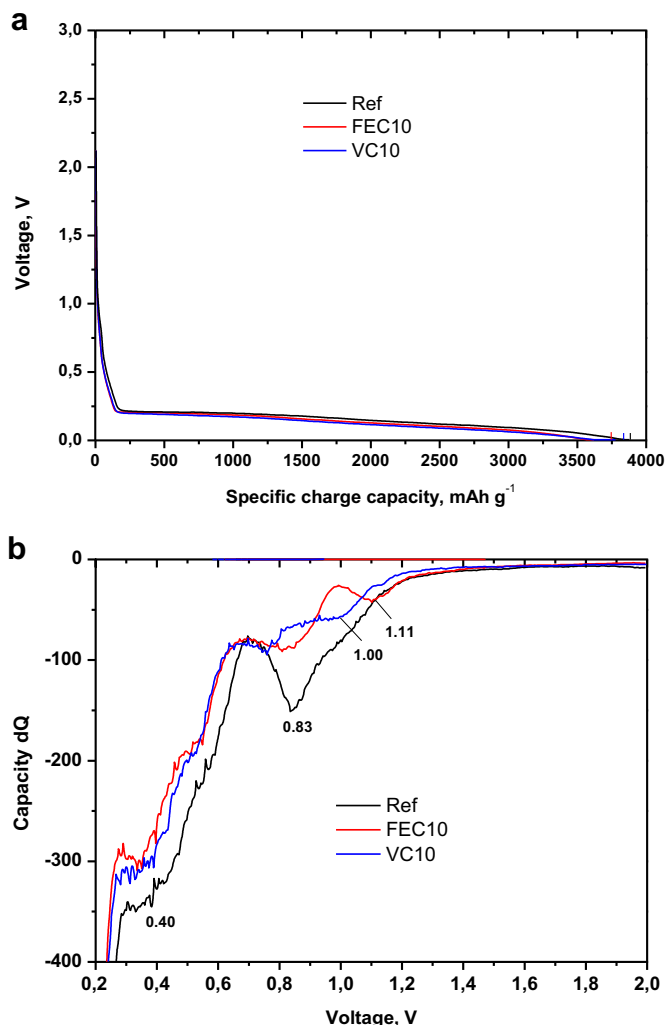| Abbreviation	EC/DEC, wt%	LiPF$_6$	Additive, wt%
Ref	3/7	1M	–
FEC10	3/7	1M	10 (FEC)
VC10	3/7	1M	10 (VC)

Fig. 1. The typical charge curves (a) and differential capacity plots (b) of the Si-based electrodes in various electrolyte solutions measured in three-electrode Swagelok cell with Li metal as a counter and reference electrodes. A constant current of 0.1 C was applied down to 5 mV, after that a constant voltage step was carried out until the current had dropped to 0.02 C.

3.2. Thermal stability and ATR-FTIR of Li$_x$Si in contact with the FEC- and VC-containing electrolytes

The thermal profiles of the lithiated silicon electrodes in contact with the electrolytes are depicted in Fig. 2. The curve presented in Fig. 2(a) has already been described in our previous work [37]. The total amount of heat generated in the region between 75 and 140 °C is markedly reduced for the electrolytes containing the additives (Fig. 2(b) and (c)). The exothermic process occurring at 123 °C ascribed to Na CMC esterification, as illustrated in Fig. 2(a) [37], is suppressed by the addition of either FEC or VC. The most remarkable feature is the shift of the main exothermic events up to values of 200 and 214 °C for the Li$_x$Si in contact with FEC10 and VC10, respectively, compared to the Li$_x$Si–Ref system, which has an onset at 153 °C, as shown in Fig. 2.

The DSC experiments were ceased at 200 °C, as shown in Fig. 2, and ATR-FTIR spectra were recorded to reveal the reasons for the thermal behavior of the Li$_x$Si–electrolyte systems at this temperature (Fig. 3(a)–(c)).

(1) Obviously, the spectrum in Fig. 3(a) differs markedly from those in Fig. 3(b) and (c). The latter two spectra are dominated
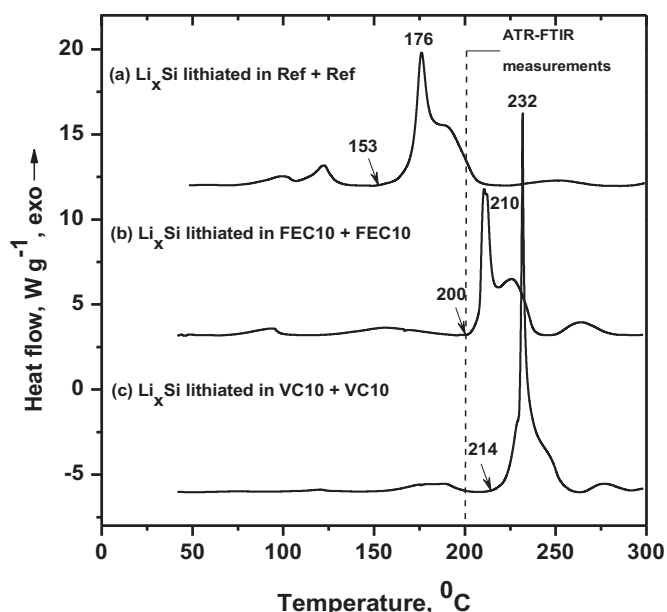
Fig. 2. The DSC profiles of Li$_x$Si heated in contact with the same electrolyte that was used for lithiation at a temperature ramp of 2 °C min^{-1}. The lithiated Si-based electrodes were rinsed in a DMC solvent and scratched off the current collector prior to DSC measurements. The dashed line indicates the temperature at which the ATR-FTIR spectra were recorded (see Fig. 3).

by extensive C=O stretching vibrations of EC at approximately 1798 and 1772 cm^{-1}. The characteristic ring stretching modes of EC can be found at 1157 and 1064 cm^{-1} in Fig. 3(b) and (c), as derived from the ATR-FTIR spectrum of EC with LiPF$_6$ in Fig. 4(a) [77,78]. In contrast, the spectrum of Li$_x$Si heated in contact with the Ref electrolyte does not show any indication of EC in Fig. 3(a). Unfortunately, the large amount of electrolyte used in the DSC experiment does not allow for a clear observation of the SEI layer decomposition when in the
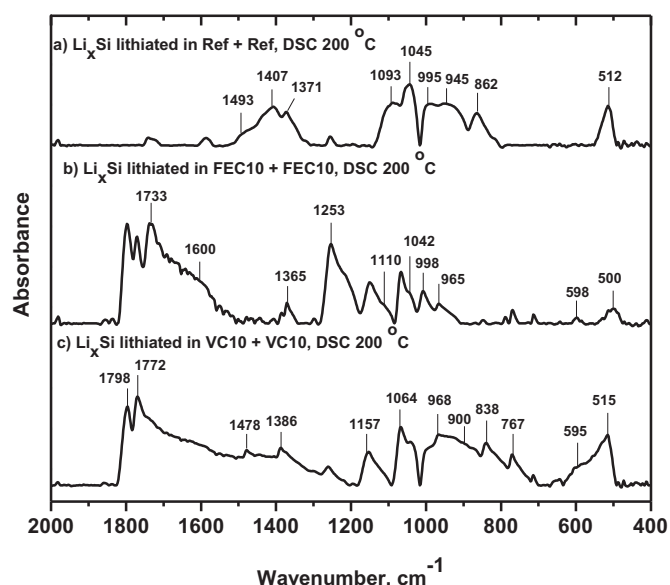

Fig. 3. The ATR-FTIR spectra of Li$_x$Si in contact with different electrolytes heated up to 200 °C. The samples were directly transferred from DSC capsules to a hermetic ATR Golden Gate unit in a glove box. The spectra were recorded under a nitrogen atmosphere with a resolution of 4 cm^{-1}.
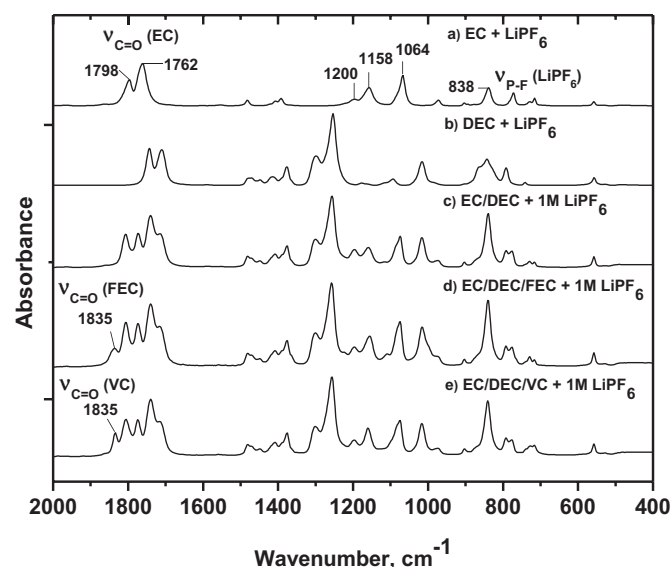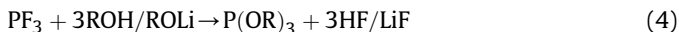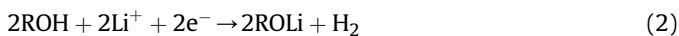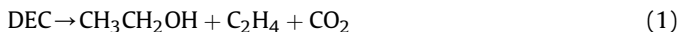

Fig. 4. The ATR-FTIR spectra of the separate solvents and electrolytes. The spectra were recorded using hermetic ATR Golden Gate unit under a nitrogen atmosphere with a resolution of 4 cm^{-1}.
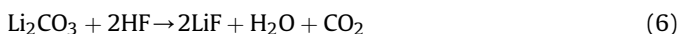
presence of FEC10 and VC10. The peaks of the polycarbonate species, which are expected as a result of the reductive decompositions of FEC and VC [58,68], may mostly overlap with the C=O stretching of EC in Fig. 3(b) and (c). The ATR-FTIR spectra of the solvents and electrolyte solutions are presented in Fig. 4.

(2) The decomposition products of the EC give rise to a group of bands at 1493, 1407 (asymmetric and symmetric C=O stretching) and 862 cm^{-1} (OCOO$^-$ bending), which correspond to Li$_2$CO$_3$ [79–81]; the other strong vibrations at 1045 (C–O–Li stretching) and 512 cm^{-1} (Li–O stretch) belong to the ROLi species in Fig. 3(a) [82,83]. The peak centered at 1093 cm^{-1} can be attributed to the Si–O stretching vibration in Fig. 3(a) [81].

(3) The Na CMC vibrations can be observed at approximately 1600 (COO$^-$ asymmetric stretching), 1110 and 1042 cm^{-1} (cellulose backbone stretching) in Fig. 3(b) and (c) [84,85], while Li$_x$Si heated in contact with the Ref electrolyte does not contain these bands (Fig. 3(a)), which implies the thermal degradation of the binder in the latter case.

(4) The features at approximately 1600 cm^{-1} are very broad in Fig. 3(b) and (c), and it is likely that several vibrational modes are overlapping in this region. The presence of unsaturated compounds with a typical C=C stretching vibration at 1600 cm^{-1} cannot be excluded for the Li$_x$Si heated in contact with FEC10 and VC10 [81].

(5) The prominent peak at 1733 cm^{-1} in Fig. 3(b), in combination with the features at 1253 and 1157 cm^{-1}, can be ascribed to the asymmetric stretching of C=O, –COO and –OCC, which are the characteristic groups of an ester [37,81]. The latter signal overlaps with the bands of EC. It is possible that esters are forming as a result of esterification of the –COONa groups of the Na CMC binder [37]. The spectrum of Li$_x$Si heated in contact with VC10 also contains small amount of esters, as shown in Fig. 3(c).

(6) The broad features between 900 and 998 cm^{-1} and at 767 cm^{-1}, which are characteristic of a P–O–C bond, are assigned to the alkyl phosphites as a result of LiPF$_6$ decompositions and further reactions with the ROH or ROLi species (Fig. 3(a)–(c)) [42,81,86]:
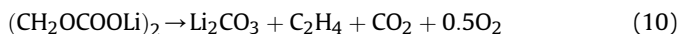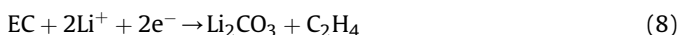
$$DEC \rightarrow CH_3CH_2OH + C_2H_4 + CO_2 \qquad (1)$$

$$2ROH + 2Li^+ + 2e^- \rightarrow 2ROLi + H_2 \qquad (2)$$

$$PF_6^- + 2e^- + 3Li^+ \rightarrow 3LiF + PF_3 \qquad (3)$$

$$PF_3 + 3ROH/ROLi \rightarrow P(OR)_3 + 3HF/LiF \qquad (4)$$

The corresponding deformation vibrations of the CH_3 and OCH_2 moieties can be found at 1365, 1386 and 1478 cm^{-1} in Fig. 3.

(7) Interestingly, the largest amount of LiF is formed on the surface of the Li_xSi heated in contact with VC10, which is confirmed by the broad peaks located at 515 and 595 cm^{-1} in Fig. 3(c) [37]. LiF can also be detected on the surface of Li_xSi when heated in contact with FEC10 (peaks at 500 and 598 cm^{-1} in Fig. 3(c)). There are several possible ways for LiF to form [42,86]:

$$LiPF_6 \leftrightarrow LiF + PF_5 \qquad (5)$$

$$Li_2CO_3 + 2HF \rightarrow 2LiF + H_2O + CO_2 \qquad (6)$$

$$Li_2CO_3 + PF_5 \rightarrow 2LiF + POF_3 + CO_2 \qquad (7)$$

In summary, it is clear that either the FEC10 and VC10 electrolytes or the SEI layers derived from those solutions prevent the thermal degradation of EC and Na CMC in the Li_xSi–electrolyte system when heated up to 200 °C. Esters, LiF, P–O–C bonds and some quantity of unsaturated compounds are predominantly formed on the surface of the lithiated Si particles when contacted with FEC10 and VC10 at elevated temperatures. On the contrary, EC and Na CMC decompose after heating the Li_xSi–Ref system up to 200 °C, which forms a large amount of Li_2CO_3, ROLi, alkyl phosphites and Si–O bonds. The following reactions may be triggered upon heating the Li_xSi–Ref system [42,87–89].

$$EC + 2Li^+ + 2e^- \rightarrow Li_2CO_3 + C_2H_4 \qquad (8)$$

$$2EC + 2Li^+ + 2e^- \rightarrow (CH_2OCOOLi)_2 + C_2H_4 \qquad (9)$$

$$(CH_2OCOOLi)_2 \rightarrow Li_2CO_3 + C_2H_4 + CO_2 + 0.5O_2 \qquad (10)$$

$$ROCOOLi \rightarrow ROLi + CO_2 \qquad (11)$$

The thermal runaway, which commenced at 153 °C in Fig. 2(a), originated from reactions between the Ref electrolyte and Li_xSi, while direct contact between the electrolyte and the lithiated electrode material was prevented in the FEC10 and VC10 solutions, as shown in Fig. 2(b) and (c), up to 200 and 214 °C, respectively.

3.3. Thermal performance and structure of the FEC- and VC-derived SEI layers

There are several possible mechanisms for protection of the lithiated nano-silicon electrodes using FEC and VC additives at elevated temperatures: (a) the formation of a thermally resistive SEI layer during the first lithiation event via reductive decomposition of the additives and (b) the generation of a protective film on the electrode surface by thermal degradation of the additives during heating. To investigate the first hypothesis, DSC measurements of the Li_xSi that was lithiated in the additive-containing electrolytes were conducted while in contact with the Ref electrolyte. Fig. 5(a) and (b) illustrate the DSC curves for the Si-based
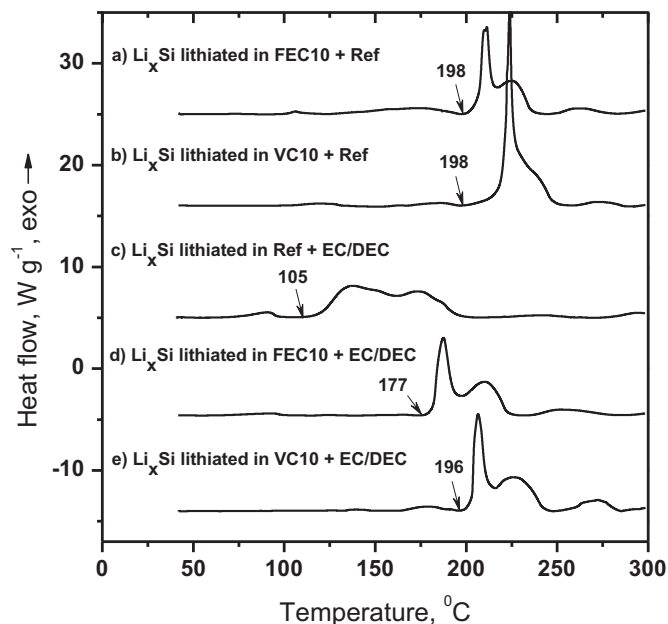

Fig. 5. The comparison between the DSC heating curves of Li_xSi in contact with additive-free electrolytes and the solvent mixtures at a temperature ramp of 2 °C min^{-1}. The lithiated Si-based electrodes were rinsed in a DMC solvent and scratched off the current collector prior to DSC measurements.

electrodes lithiated in either FEC10 or VC10. The electrodes were then washed in a DMC solvent, dried under vacuum and sealed in a DSC pan with the Ref electrolyte. The intensities of the thermal reactions appeared to decrease in temperatures up to 150 °C, and the main exothermic events occurred at substantially higher temperatures (above 198 °C) compared to the Li_xSi lithiated in the Ref electrolyte, which experienced an onset temperature of 153 °C (Fig. 2(a)). This result can be explained by the development of a protective coating of FEC- and VC-derived SEI layers on the surface of the lithiated Si-based electrode. Previously, it was found that EC/DEC solvent mixtures can trigger the thermal degradation of Li_xSi when cycled in a Ref electrolyte at approximately 105 °C, as shown in Fig. 5(c) [37]. To further investigate the properties of the FEC- and VC-derived SEI layers on the surface of the Li_xSi electrodes, their thermal stability was measured while in the EC/DEC solvents, as shown in Fig. 5(d) and (e). It can be seen that the intense exothermic reactions commence at 177 and 196 °C for the Si-based electrodes lithiated in FEC10 and VC10, respectively, which confirms the thermal resistivity of the FEC- and VC-derived SEI layers.

The ATR-FTIR spectra of the Si-based electrodes recorded after the first cycle provided information on the surface chemistry, which was derived from either the additive-free electrolyte or a VC- or FEC-containing electrolyte, and are shown in Fig. 6. All spectra presented in Fig. 6 contain features that correspond to Na CMC (1609, 1407 and 1020–930 cm^{-1}) [84,85]. The suppression of the broad peaks in the approximate range of 1200–1100 cm^{-1} (Fig. 6(a)) following one cycle in each of the electrolytes reflects the electrochemical modification of the silicon oxide native layer on the surface of the silicon nano-particles. Strong vibrations of the $OCOO^-$ moiety of the Li_2CO_3 at 1500, 1407 and 867 cm^{-1} can be found for all three electrodes in Fig. 6(b)–(d) [79–81]. Several specific features can be identified in the spectra of the Si-based electrodes that were measured in different electrolytes:

(1) The lithium alkyl carbonates are characterized by bands at 1698, 1650 (C=O asymmetric stretching), 1443 (CH_2 bending),
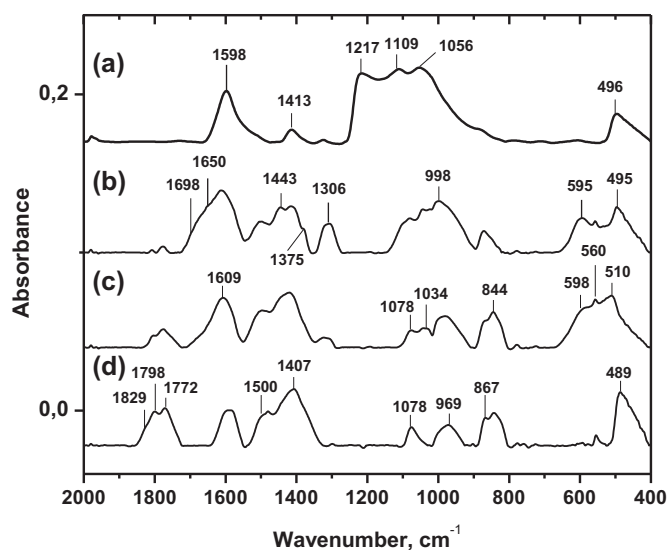
Fig. 6. The ATR-FTIR spectra of a pristine Si-based electrode (a) and the same electrode after one cycle in (b) Ref, (c) FEC10 and (d) VC10. The lithiated Si-based electrodes were rinsed in a DMC solvent prior to spectroscopic measurements. The spectra were recorded under a nitrogen atmosphere with a resolution of 4 cm^{-1}.

1375 (CH$_3$ symmetric deformation), 1306 (C=O symmetric stretching), 1078, 1034 (C–O stretching), 867 (OCOO$^-$ bending) and 595 cm^{-1} (Li–O stretching) [58,82,89,90]. These carbonates form on the Si particle surfaces in the Ref electrolyte as the main component of the SEI layer (Fig. 6(b)). A very small amount of ROCOOLi can be observed for the Si-based electrode cycled in FEC10. In addition, no traces of those compounds can

be detected on the surface of the electrode cycled in VC10 (Fig. 6(c) and (d)).

(2) The reductive decomposition of the FEC additive resulted in the formation of a large amount of LiF (598 and 510 cm^{-1}) on the Si-based electrode surface as shown in Fig. 6(c).

(3) The group of peaks located at 1772–1829 cm^{-1} in Fig. 6(c) and (d) results from the C=O stretching modes of the polycarbonate species that is derived from the electrochemical decomposition of the VC and FEC. This finding is in agreement with other works [58,68,91]. The C=O vibrations of EC can also be observed in this region, as shown in Fig. 4. However, the disappearance of the fundamental ring vibrational modes of EC, which should be visible at 1200 and 1158 cm^{-1}, proved the absence of ethylene carbonate in the electrodes under investigation [77,78].

Based on the ATR-FTIR spectra and the DSC analyses of the Si-based electrodes cycled in the Ref, FEC10 and VC10 electrolytes, we conclude that the lithium alkyl carbonates, which are the main decomposition product of EC, cause the development of a thermally unstable film on the surface of the Si particles. Lithium organic carbonates are metastable components of the SEI layer and are capable of converting to Li$_2$CO$_3$ or ROLi at elevated temperatures, according to Eqs. (10) and (11). Because of this, they do not provide a thermally robust protective layer on the surfaces of the lithiated Si nano-particles. The thermally destroyed porous SEI layer is then permeable to the electrolyte components, and interaction between the electrolyte and Li$_x$Si occurs at 153 °C, as presented in Fig. 2(a) and, schematically, in Fig. 7, route A. In contrast, polymerization of VC and FEC on the Si particle surfaces in the FEC and VC10 electrolytes creates a compact SEI layer that contains polycarbonate species, which possess an enhanced thermal stability. The mechanism of reductive decomposition of FEC includes both the
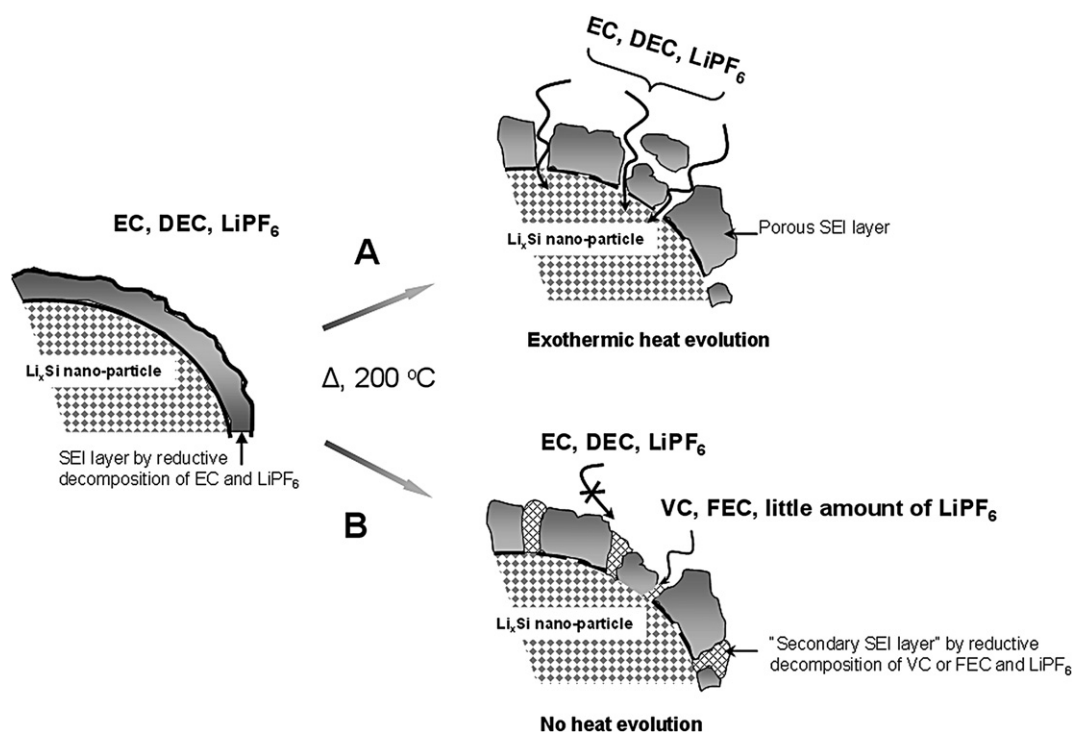

Fig. 7. A schematic diagram showing the thermal events in the Li$_x$Si–Ref system that occur while heating up to 200 °C (route A). Thermal degradation of the SEI layer makes it porous and permeable to the electrolyte components, such as EC, DEC, and LiPF$_6$. Direct contact between the components and Li$_x$Si initiates the thermal runaway. The thermal reactions of Li$_x$Si that was lithiated in the Ref electrolyte, washed, dried and heated in contact with either FEC10 or VC10 are shown in route B. Upon thermal degradation, the FEC and VC additives in contact with Li$_x$Si provide the "secondary SEI" layer, which does not allow direct interaction between Li$_x$Si and the electrolyte.

elimination of HF in the first step to produce the VC and subsequent electrochemical polymerization of VC. This mechanism was first proposed by Aurbach et al. [57]. That is, the electrochemical reduction of either FEC or VC leads to the similar compositions of the SEI layers derived from the FEC- or VC-containing electrolyte solutions so that polycarbonates are formed in both cases. Our results confirm that polycarbonate-based SEI layers effectively prevent direct contact between Li_xSi and the electrolyte while heating to 198 °C (Fig. 5(a) and (b)). The layers also prevent contact between Li_xSi and the EC/DEC solvent mixture up to 177 and 196 °C (Fig. 5(d) and (e)). In addition, LiF generated on the electrode cycled in FEC10, which increases the thermal resistivity of the protective surface film [75]. Fig. 8 illustrates a schematic representation of the mechanism of Si nano-particle protection by the FEC- and VC-derived SEI layers at elevated temperatures.

Comparison of the DSC results obtained in presence of the FEC and VC electrolyte additives in Figs. 2 (b), (c) and 5(a), (b) shows that the use of VC results in slightly higher onset temperatures of the exothermic events. This can be due to more effective, SEI layer with a different composition, thickness, or density formed in the presence of the VC additive. At the same time, the peak centered at around 232 °C for the VC-containing system is particularly sharp and intensive. This may indicate that the VC-derived SEI layer is effective only at temperatures below 200 °C while further heating of the sample results in a more violent exothermal reaction. At contrast, the FEC-derived SEI demonstrates protective properties in the entire temperature range.

3.4. Effect of FEC and VC additives on the thermal stability of the Li_xSi–electrolyte system

To investigate whether the free FEC and VC additives present in the electrolyte solutions influenced the thermal stability of the fully lithiated nano-Si electrode, DSC measurements were conducted for the Li_xSi that was lithiated in the Ref electrolyte and then heated with the additive-containing solutions. After full lithiation in the Ref electrolyte, the Si-based electrodes were retrieved and rinsed in the DMC, dried under vacuum and sealed in a DSC pan with FEC10 or VC10. This experiment completely excludes the influence of the FEC- or VC-derived SEI layers on the thermal resistivity of Li_xSi in contact with the electrolytes. Fig. 9(a) and (b) clearly show the onset temperatures of the main exothermic events to be 209 and 204 °C when FEC and VC, respectively, are used as additives. The excellent thermal stability of Li_xSi was demonstrated when in contact with FEC10 and VC10 versus the Li_xSi–Ref system (shown in Fig. 2(a)). This important result implies that FEC and VC generate a robust "secondary SEI layer" on the surface of the lithiated Si nano-particles at elevated temperatures, which cures the thermo-dynamically unstable SEI layer that forms electrochemically in the Ref electrolyte during the first charge, as shown in Fig. 7, route B.
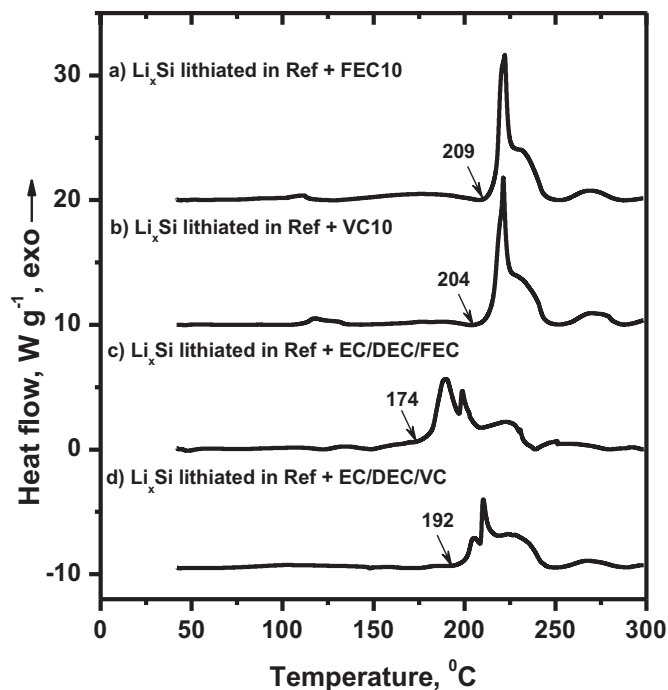
Fig. 9. The DSC heating curves for Li_xSi lithiated in the Ref electrolyte and then heated in contact with various electrolytes and solvent mixtures at a temperature ramp of 2 °C min^{-1}. The lithiated Si-based electrodes were rinsed in a DMC solvent and scratched off the current collector. DSC measurements were performed in a high-pressure hermetic stainless steel pans.

We propose that, due to the increased reactivity of the FEC and VC versus the EC, the additives interact immediately with the newly exposed Li_xSi surfaces during the thermal degradation process of the metastable SEI layer, which occurs upon heating to yield the polycarbonates. The "secondary SEI layer" consists mostly of polymeric species and effectively protects the Li_xSi particles from direct reactions with the main electrolyte components EC, DEC and LiPF$_6$.

We have discussed such a "repair mechanism" of the SEI in previous works with Sn-based lithium storage alloys [40]. We proposed a model for the formation of a "secondary SEI" repairing the holes in the "primary SEI"; the holes being a result of crack formation in the underlying lithium storage metal host due to strong volume expansion. In that case, the "secondary SEI" was formed by an electrochemical reaction with the electrolyte. In this work it is formed by a thermal reaction. From the previous work [40], the authors are aware, that in addition to an increased reactivity of the Li_xSi with the electrolyte at elevated temperatures, also the volume changes induced by elevated temperatures, for instance by Li loss from Li_xSi due to reaction with the electrolyte might play
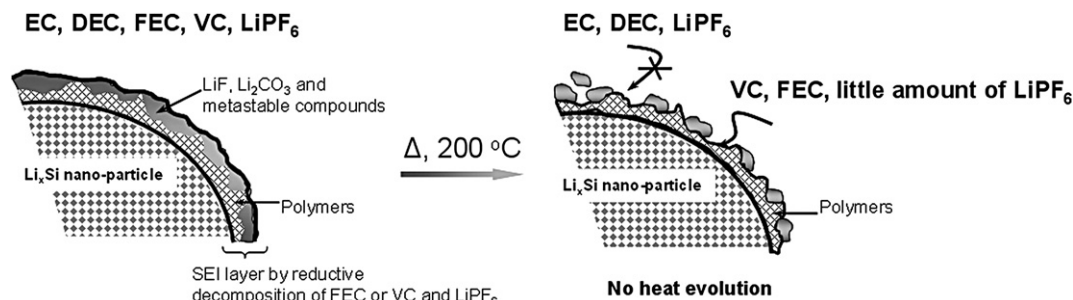
Fig. 8. A schematic diagram showing the protective function of the FEC- and VC-derived SEI layers on the surface of the lithiated Si nano-particles during heating up to 200 °C. The SEI layer, which forms electrochemically, is mostly composed of a polymer species and shows excellent stability at elevated temperatures.

a role for the observed phenomena in particular as such reactions depend on the electrolyte composition.

3.5. The influence of $LiPF_6$ on the thermal behavior of Li_xSi in contact with the FEC- and VC-containing solvent mixtures

The role of the $LiPF_6$ salt in thermal reactions between the FEC- and VC-containing electrolytes in contact with Li_xSi might have special significance because this electrolyte component is unstable at temperatures above 70 °C and is usually used in high concentrations [92–94]. Fig. 9(c) and (d) illustrate the DSC thermal profiles of fully lithiated silicon electrodes heated in contact with the EC/DEC/FEC or EC/DEC/VC solvent mixtures. It should be noted that some traces of $LiPF_6$ may be present in the samples because complete removal of the salt may be not possible by rinsing the electrodes in DMC after lithiation. However, the DSC heating curves collected in the presence of $LiPF_6$ and without the salt differ markedly from each other. Elimination of the $LiPF_6$ salt causes broadening of the DSC signals and lowers the onset temperature of the intense exothermic reactions. Thus, the main exothermic event occurs after 174 °C for the system of Li_xSi–EC/DEC/FEC; however, for the Li_xSi–FEC10 system, this event does not occur until 209 °C. A similar situation exists for the system of Li_xSi–EC/DEC/VC, which evolves the largest amount of heat after 192 °C, while Li_xSi–VC10 showed an onset temperature of 204 °C in Fig. 9. Clearly, the $LiPF_6$ salt takes part in the formation of the "secondary SEI layer" in a process that shifts the onset temperatures of the intense heat evolved by the Li_xSi–electrolyte systems to higher values. Whereas the decomposition of $LiPF_6$ at high temperatures usually results in fast capacity and power fade [95], $LiPF_6$ appears to be useful for enhancing the thermal stability of the interface between the lithiated silicon particles and the electrolytes during heating. The PF_6^- anion can be reduced electrochemically with FEC and VC upon exposure of fresh Li_xSi surfaces during the thermal degradation of the initial unstable SEI layer, as shown in Eq. (3). Due to its excellent thermal properties, LiF increases the stability of SEI layers at elevated temperatures [75,96].

However, the thermal protection function of $LiPF_6$ is more complex and selective in terms of the electrode active material. Fig. 10 illustrates the DSC heating curves for Li metal heated in contact with FEC10, VC10 and with solvent mixtures without the salt. It can be seen that the presence of $LiPF_6$ reduces the onset temperatures of the exothermic reactions between the electrolytes and Li metal, as shown in Fig. 10. This same tendency was observed in our previous study on Li metal heated with a Ref electrolyte, where the onset occurred at approximately 170 °C with EC/DEC and the exothermic reactions started at 189 °C [37]. Here, we relate the observed phenomena to the ability of silicon to utilize HF, which is highly reactive and forms as a product of the thermal degradation of $LiPF_6$:

$$PF_5 + H_2O \rightarrow POF_3 + 2HF \quad (12)$$

$$SiO_x + 4HF + 2F^- \rightarrow SiF_6^{2-} + xH_2O \quad (13)$$
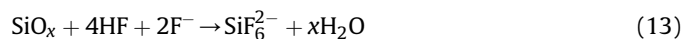
It is known that the formation of silicon oxides is unavoidable during the cycling of silicon electrodes [65,67]. Due to its high bonding energy, the Si–F bond (565 kJ mol^{-1}) is stable even at elevated temperatures, but the Si–O bond (452 kJ mol^{-1}) is not [66]. Therefore, the harmful influence of HF – which is responsible for a large number of the exothermic reactions that occur in LIBs [42,89,97] – is neutralized by interaction with the silicon active material. The thermal resistivity of the Li_xSi–electrolyte interface is enhanced in the presence of $LiPF_6$ because of the utilization of HF. In
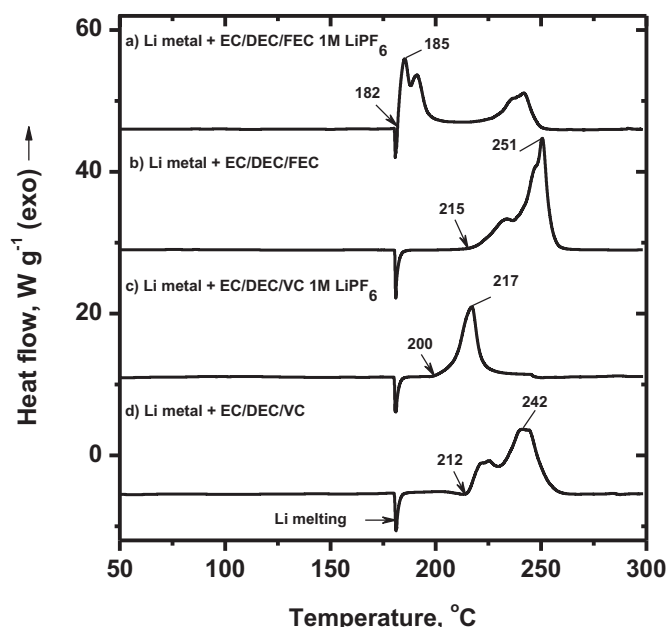

Fig. 10. The DSC profiles of Li metal heated in contact with different electrolytes and solvent mixtures at a temperature ramp of 2 °C min^{-1}. DSC measurements were performed in a high-pressure hermetic stainless steel pans.

contrast, the Li metal–electrolyte interface suffers an early thermal runaway caused by the introduction of $LiPF_6$ into the electrolyte.

4. Conclusion

The thermal stability of a fully lithiated nano-silicon electrode when heated in contact with an EC/DEC 1 M $LiPF_6$ electrolyte was investigated in the absence and presence of 10 wt.% FEC and VC additives. The results indicate that the electrolyte additives play crucial roles in enhancing the thermal stability of the SEI at elevated temperatures. Thus, Li_xSi lithiated in FEC10 or VC10 and then heated with the same electrolyte shows no considerable thermal events up to 200 °C and 214 °C, respectively, whereas the Li_xSi–Ref system suffers an earlier thermal degradation, which commences at 153 °C. The mechanism for protecting lithiated silicon in contact with an electrolyte by incorporating FEC and VC additives was thoroughly studied. It was found that the SEI layer formed electrochemically on the Si nano-particle surfaces via reductive decomposition of the additives and that the free FEC or VC in the electrolyte solution is capable of protecting the Li_xSi from violent exothermic reactions with the electrolyte components at elevated temperatures. The ATR-FTIR analysis of the "primary SEI", which is formed on the surface of the Si electrode when charged in different electrolytes, revealed the presence of a polycarbonate species in the FEC and VC 10 electrolytes, whereas the Ref solution produced metastable lithium alkyl carbonates as the main "primary SEI" components. The polycarbonates were found to be responsible for an enhanced thermal stability of the Li_xSi with the electrolyte. Moreover, the ability of FEC and VC to immediately polymerize when in contact with the newly exposed Li_xSi at elevated temperatures leads to the creation of a robust "secondary SEI", which repairs any cracks and pores in the "primay SEI". This accounts for the positive effect of the free additives on the thermal stability of the Li_xSi (SEI layer formed in Ref electrolyte) with FEC10 or VC10. Despite its well-known detrimental effect on the electrochemical performance at elevated temperature, the $LiPF_6$ salt appeared to be useful for increasing the onset temperature of the thermal

reactions between Li$_x$Si and the electrolytes to higher values in the presence of the additives.

References

[1] M. Winter, S. Passerini, in: Energy Conference (INTELEC), IEEE 33rd International, IEEE, 2011, ISBN 978-1-4577-1249-4, pp. 1–3.
[2] M. Winter, S. Passerini, Fortschritt-Berichte VDI, Reihe 12, Issue 735-2, in: 32nd International Vienna Motor Symposium (5–6 May 2011), pp. 82–85.
[3] M. Winter, J.O. Besenhard, Chemie in unserer Zeit 33 (1999) 320–332.
[4] J.O. Besenhard, M. Winter, Pure and Applied Chemistry 70 (1998) 603–608.
[5] G.H. Wrodnigg, T.M. Wrodnigg, J.O. Besenhard, M. Winter, Electrochemistry Communications 1 (1999) 148–150.
[6] G.H. Wrodnigg, J.O. Besenhard, M. Winter, Journal of Power Sources 97, 98 (2001) 592–594.
[7] R. Schmitz, R.W. Schmitz, R. Müller, O. Kazakova, N. Kallinovich, G.-V. Röschenthaler, M. Winter, S. Passerini, A. Lex-Balducci, Journal of Power Sources 205 (2012) 408–413.
[8] P. Isken, C. Dippel, R. Schmitz, R.W. Schmitz, M. Kunze, S. Passerini, M. Winter, A. Lex-Balducci, Electrochimica Acta 56 (2011) 7530–7535.
[9] T. Nagaura, in: Proceedings of the 5th International Seminar on Lithium Battery Technology and Applications, Deerfield Beach, FL, Florida Educational Seminars, Inc., Boca Raton, FL, March 5–7, 1990.
[10] P.G. Balakrishnan, R. Ramesh, T. Prem Kumar, Journal of Power Sources 155 (2006) 401–414.
[11] M. Sternad, M. Cifrain, D. Watzenig, G. Brasseur, M. Winter, e&i Elektrotechnik und Elektronik 126 (2009) 186–193.
[12] D. Lisbona, T. Snee, Process Safety and Environmetal Protection 89 (2011) 434–442.
[13] Q. Wang, P. Ping, X. Zhao, G. Chu, J. Sun, C. Chen, Journal of Power Sources 208 (2012) 210–224.
[14] M. Winter, J.O. Besenhard, Electrochimica Acta 45 (1999) 31–50.
[15] A. Trifonova, M. Wachtler, M.R. Wagner, H. Schroettner, Ch. Mitterbauer, F. Hofer, K.-C. Möller, M. Winter, J.O. Besenhard, Solid State Ionics 168 (2004) 51–59.
[16] M. Wachtler, M. Winter, J.O. Besenhard, Journal of Power Sources 105 (2002) 151–160.
[17] J.O. Besenhard, M. Wachtler, M. Winter, R. Andreaus, I. Rom, W. Sitte, Journal of Power Sources 81, 82 (1999) 268–272.
[18] M. Wachtler, M.R. Wagner, M. Schmied, M. Winter, J.O. Besenhard, Journal of Electroanalytical Chemistry 510 (2001) 12–19.
[19] A. Trifonova, M. Winter, J.O. Besenhard, Journal of Power Sources 174 (2007) 800–804.
[20] A. Trifonova, M. Wachtler, M. Winter, J.O. Besenhard, Ionics 8 (2002) 321–328.
[21] M.N. Obrovac, L. Christensen, Electrochemical and Solid-State Letters 7 (2004) A93–A96.
[22] J.R. Szczech, S. Jin, Energy & Environmental Science 4 (2011) 56–72.
[23] W.-J. Zhang, Journal of Power Sources 196 (2011) 13–24.
[24] U. Kasavajjula, C. Wang, A.J. Appleby, Journal of Power Sources 163 (2007) 1003–1039.
[25] P.G. Bruce, B. Scrosati, J.M. Tarascon, Angewandte Chemie International Edition 47 (2008) 2930–2946.
[26] A.S. Aricò, P. Bruce, B. Scrosati, J.-M. Tarascon, W. van Schalkwijk, Nature Materials 4 (2005) 366–377.
[27] P.R. Raimann, N.S. Hochgatterer, C. Korepp, K.C. Möller, M. Winter, H. Schröttner, F. Hofer, J.O. Besenhard, Ionics 12 (2006) 253–255.
[28] M. Winter, M. Wachtler, J. Yang, J.H. Albering, B. Evers, I. Schneider, F. Hofer, I. Papst, J.O. Besenhard, ITE Battery Letters 1 (1999) 140–149.
[29] M. Winter, J.O. Besenhard, J.H. Albering, J. Yang, M. Wachtler, Progress in Batteries and Battery Materials 17 (1998) 208–213.
[30] J. Cho, Journal of Material Chemistry 20 (2010) 4009–4014.
[31] A.R. Kamali, D.J. Fray, Journal of New Materials for Electrochemical Systems 160 (2010) 147–160.
[32] W.R. Liu, N.-L. Wu, D.-T. Shieh, H.-C. Wu, M.H. Yang, C. Korepp, J.O. Besenhard, M. Winter, Journal of Electrochemical Society 154 (2007) A97–A102.
[33] W.R. Liu, Y.-C. Yen, H.-C. Wu, M. Winter, N.-L. Wu, Journal of Applied Electrochemistry 39 (2009) 1643–1649.
[34] M. Schmuck, A. Balducci, B. Rupp, W. Kern, S. Passerini, M. Winter, Journal of Solid State Electrochemistry 14 (2010) 2203–2207.
[35] N.S. Hochgatterer, M.R. Schweiger, S. Koller, P.R. Raimann, T. Wöhrle, C. Wurm, M. Winter, Electrochemical and Solid-State Letters 11 (2008) A76–A80.
[36] Y.-S. Park, S.-M. Lee, Bulletin of the Korean Chemical Society 32 (2011) 145–148.
[37] I.A. Profatilova, T. Langer, J.P. Badillo, A. Schmitz, H. Orthner, H. Wiggers, S. Passerini, M. Winter, Journal of Electrochemical Society 159 (2012) A657–A663.
[38] M.R. Wagner, P.R. Raimann, K.C. Möller, J.O. Besenhard, M. Winter, Analytical and Bioanalytical Chemistry 379 (2004) 272–276.
[39] M.R. Wagner, P. Raimann, K.-C. Möller, J.O. Besenhard, M. Winter, Electrochemical and Solid-State Letters. 7 (2004) A201–A205.
[40] M. Wachtler, J.O. .Besenhard, M. Winter, Journal of Power Sources 94 (2001) 189–193.
[41] M. Winter, W.K. Appel, B. Evers, T. Hodal, K.-C. Möller, I. Schneider, M. Wachtler, M.R. Wagner, G.H. Wrodnigg, J.O. Besenhard, Monatshefte für Chemie 132 (2001) 473–486.
[42] P.B. Balbuena, Y. Wang (Eds.), Lithium-Ion Batteries, Solid–Electrolyte Interphase, Imperial College Press, London, 2004. 407 pp.
[43] M. Winter, Zeitschrift fuer Physikalische Chemie 223 (2009) 1395–1406.
[44] M. Winter, H. Buqa, B. Evers, T. Hodal, K.-C. Möller, C. Reisinger, M.V. Santis Alvarez, I. Schneider, G.H. Wrodnigg, F.P. Netzer, R.I.R. Blyth, M.G. Ramsey, P. Golob, F. Hofer, C. Grogger, W. Kern, R. Saf, J.O. Besenhard, ITE Battery Letters 1, 2 (1999) 129–139.
[45] Y. Oumellal, N. Delpuech, D. Mazouzi, N. Dupre, J. Gaubicher, P. Moreau, P. Soudan, B. Lestriez, D. Guardyom, Journal of Material Chemistry 21 (2011) 6201–6208.
[46] M.R. Wagner, J.H. Albering, K.C. Möller, J.O. Besenhard, M. Winter, Electrochemical Communications 7 (2005) 947–952.
[47] K. Tasaki, A. Goldberg, M. Winter, Electrochimica Acta 56 (2011) 10424–10435.
[48] J.O. Besenhard, M.W. Wagner, M. Winter, A.D. Jannakoudakis, P.D. Jannakoudakis, E. Theodoridou, Journal of Power Sources 44 (1993) 413–420.
[49] G.H. Wrodnigg, J.O. Besenhard, M. Winter, Journal of Electrochemical Society 146 (1999) 470–472.
[50] C. Korepp, W. Kern, E.A. Lanzer, P.R. Raimann, J.O. Besenhard, M. Yang, K.-C. Möller, D.-T. Shieh, M. Winter, Journal of Power Sources 174 (2007) 628–631.
[51] C. Korepp, H.J. Santner, T. Fuji, M. Ue, J.O. Besenhard, K.C. Möller, M. Winter, Journal of Power Sources 158 (2006) 578–582.
[52] C. Korepp, K.-C. Möller, D.-T. Shieh, J.O. Besenhard, M.H. Yang, M. Winter, Journal of Power Sources 174 (2007) 387–393.
[53] K. Xu, Chemical Reviews 104 (2004) 4303–4417.
[54] S.S. Zhang, Journal of Power Sources 162 (2006) 1379–1394.
[55] R. McMillan, H. Slegr, Z.X. Shu, W. Wang, Journal of Power Sources 81, 82 (1999) 20–26.
[56] R. Mogi, M. Inaba, S.-K. Jeong, Y. Iriyama, T. Abe, Z. Ogumi, Journal of Electrochemical Society 149 (2002) A1578–A1583.
[57] D. Aurbach, K. Gamolsky, B. Markovsky, Y. Gofer, M. Schmidt, U. Heider, Electrochimica Acta 47 (2002) 1423–1439.
[58] H. Ota, Y. Sakata, A. Inoue, S. Yamaguchi, Journal of Electrochemical Society 151 (2004) A1659–A1669.
[59] E.-G. Shim, T.-H. Nam, J.-G. Kim, H.-S. Kim, S.-I. Moon, Journal of Power Sources 172 (2007) 901–907.
[60] O. Matsuoka, A. Hiwara, T. Omi, M. Toriida, T. Hayashi, C. Tanaka, Y. Saito, T. Ishida, H. Tan, S.S. Ono, S. Yamamoto, Journal of Power Sources 108 (2002) 128–138.
[61] S.K. Jeong, M. Inaba, R. Mogi, Y. Iriyama, T. Abe, Z. Ogumi, Langmuir 17 (2001) 8281–8286.
[62] N.-S. Choi, Y. Lee, S.-S. Kim, S.-C. Shin, Y.-M. Kang, Journal of Power Sources 195 (2010) 2368–2371.
[63] L. El Ouatani, R. Dedryvère, C. Siret, P. Biensan, S. Reynaud, P. Iratçabal, D. Gonbeau, Journal of Electrochemical Society 156 (2009) A103–A113.
[64] C.-C. Chang, S.-H. Hsu, Y.-F. Jung, C.-H. Yang, Journal of Power Sources 196 (2011) 9605–9611.
[65] L. Chen, K. Wang, X. Xie, J. Xie, Journal of Power Sources 174 (2007) 538–543.
[66] N.-S. Choi, K.H. Yew, K.Y. Lee, M. Sung, H. Kim, S.-S. Kim, Journal of Power Sources 161 (2006) 1254–1259.
[67] H. Nakai, T. Kubota, A. Kita, A. Kawashima, Journal of Electrochemical Society 158 (2011) A798–A801.
[68] V. Etacheri, O. Haik, Y. Goffer, G.A. Roberts, I.C. Stefan, R. Fasching, D. Aurbach, Langmuir 28 (2012) 965–976.
[69] K. Abe, H. Yoshitake, T. Kitakura, T. Hattori, H. Wang, M. Yoshio, Electrochimica Acta 49 (2004) 4613–4622.
[70] M. Winter, R. Imhof, F. Joho, P. Novák, Journal of Power Sources 81, 82 (1999) 818–823.
[71] M. Winter, P. Novák, Journal of Electrochemical Society 145 (1998) L27–L30.
[72] M. Herstedt, H. Rensmob, H. Siegbahn, K. Edström, Electrochimica Acta 49 (2004) 2351–2359.
[73] H.-H. Lee, Y.-Y. Wang, C.-C. Wan, M.-H. Yang, H.-C. Wu, D.-T. Shieh, Journal of Applied Electrochemistry. 35 (2005) 615–623.
[74] M.-H. Ryou, G.-B. Han, Y.M. Lee, J.-N. Lee, D.J. Lee, Y.O. Yoon, J.-K. Park, Electrochimica Acta 55 (2010) 2073–2077.
[75] I.A. Profatilova, S.-S. Kim, N.-S. Choi, Electrochimica Acta 54 (2009) 4445–4450.
[76] I.A. Profatilova, N.-S. Choi, S.W. Roh, S.S. Kim, Journal of Power Sources 192 (2009) 636–643.
[77] B. Fortunato, Spectrochimica Acta 27A (1971) 1917–1927.

[78] P.A. Brooksby, W.R. Fawcett, Spectrochimica Acta, Part A 57 (2001) 1207−1221.
[79] M.H. Brooker, J.B. Bates, Journal of Chemical Physics 54 (1971) 4788−4796.
[80] Y. Ein-Eli, S.F. McDevitt, B. Markovsky, A. Schechter, D. Aurbach, Journal of Electrochemical Society 144 (1997) L180−L184.
[81] G. Socrates, in: Infrared and Raman Characteristic Group Frequencies, third ed. John Wiley & Sons, New York, 2001.
[82] S. Matsuta, T. Asada, K. Kitaura, Journal of Electrochemical Society 147 (2000) 1695−1702.
[83] D. Aurbach, M.L. Daroux, P.W. Faguy, E. Yeager, Journal of Electrochemical Society 135 (1988) 1863−1871.
[84] L.T. Cuba-Chiem, L. Huynh, J. Ralston, D.A. Beattie, Minerals Engineering 21 (2008) 1013−1019.
[85] J.-J. Max, C. Chapados, Journal of Physical Chemistry A 108 (2004) 3324−3337.
[86] J.S. Gnanaraj, E. Zinigrad, L. Asraf, H.E. Gottlieb, M. Sprecher, M. Schmidt, W. Geissler, D. Aurbach, Journal of Electrochemical Society 150 (2003) A1533−A1537.
[87] C.L. Campion, W. Li, B.L. Lucht, Journal of Electrochemical Society 152 (2005) A2327−A2334.
[88] O. Haik, S. Ganin, G. Gershinsky, E. Zinigrad, B. Markovsky, D. Aurbach, I. Halalay, Journal of Electrochemical Society 158 (2011) A913−A923.
[89] G.V. Zhuang, H. Yang, P.N. Ross, J.K. Xu, T.R. Jow, Electrochemical and Solid-State Letters 9 (2006) A64−A68.
[90] Von W. Behrendt, G. Gattow, M. Drager, Zeitschrift für anorganische und allgemeine Chemie 397 (1973) 237−246.
[91] J.-S. Bridel, S. Grugeon, S. Laruelle, J. Hassoun, P. Reale, B. Scrosati, J.-M. Tarascon, Journal of Power Sources 195 (2010) 2036−2043.
[92] B. Ravdel, K.M. Abraham, R. Gitzendanner, J. DiCarlo, B. Lucht, C. Campion, Journal of Power Sources 119−121 (2003) 805−810.
[93] Z. Lu, L. Yang, Y. Guo, Journal of Power Sources 156 (2006) 555−559.
[94] L. Terborg, S. Nowak, S. Passerini, M. Winter, U. Karst, P.R. Haddad, P.N. Nesterenko, Analytica Chimica Acta 714 (2012) 121−126.
[95] S.F. Lux, I.T. Lucas, E. Pollak, S. Passerini, M. Winter, R. Kostecki, Electrochemical Communications 14 (2012) 47−50.
[96] Y. Wang, J.R. Dahn, Journal of Electrochemical Society 153 (2006) A2188−A2191.
[97] I.A. Profatilova, N.-S. Choi, K.H. Yew, W.-U. Choi, Solid State Ionics 179 (2008) 2399−2405.